Chapter 9
Sediment–Water Interfaces, Chemical Flux at

Louis J. Thibodeaux and Joseph Germano

Glossary

Benthic boundary layer	A slow moving water layer above the sediment.
Bioturbation transport	A chemical mobility process driven by the presence of macrofauna and macroflora residing near the interface.
Chemical flux	The basic term that quantifies chemical mobility across an interface with units of mass per area per time ($kg/m^2/s$)
Chemical mobility	A general term used to denote the idea that chemicals do move from place to place.
Interface	A real or imaginary plane which separates water from sediment.
Mass transfer rate	The chemical flux times the area perpendicular to its direction of movement (kg/s).
Sediment surface layers	A series of distinctive mud layers occupying thickness of several centimeters depth.
Transport model	One of several concepts for describing a chemical mobility process, and the associated formula or algorithm needed to describe it mathematically (a.k.a., the flux expression).

This chapter was originally published as part of the Encyclopedia of Sustainability Science and Technology edited by Robert A. Meyers. DOI:10.1007/978-1-4419-0851-3

L.J. Thibodeaux (✉)
Cain Department Chemical Engineering, Louisiana State University, Baton Rouge, LA 70820, USA
e-mail: thibod@lsu.edu

J. Germano
Germano & Associates, Inc., 12100 SE 46th Place, Bellevue, WA 98006, USA
e-mail: joe@remots.com

J.S. Gulliver (ed.), *Transport and Fate of Chemicals in the Environment: Selected Entries from the Encyclopedia of Sustainability Science and Technology*,
DOI 10.1007/978-1-4614-5731-2_9,

Definition of the Subject

Numerous individual transport processes which mobilize chemicals on either side of the interface have been studied. However, a consistent theoretical framework connecting the processes across the interface that correctly quantifies the overall flux remains elusive. This occurs because two fundamentally different individual flux relationships are needed to represent the two very different transport mechanisms needed for quantifying the numerous chemical, biological, and physical processes ongoing at this unique locale. The two basic types of transport processes are the chemical potential driven and the media advection driven. Several theoretical modeling approaches exist for combining these, but all have problematic conceptual features, which will be reviewed. By generalizing flux continuity across the interface, which is the fundamental basis for arriving at the well-known and accepted two-resistance theory, the "interface compartment model" is presented and offered as a unifying theory describing advection-driven and potential-driven transport across the sediment–water interface.

Introduction

All theories for chemical transport across the interface originate from the nineteenth century with the Ohm–Kirchhoff laws of electrical currents and potentials. Lewis and Whitman [1] used an analogous electrical flux approach for deriving the chemical potential–driven flux across a gas–liquid interface. It is presumed that most of the significant, individual chemical transport processes on both sides of the sediment–water interface, which influence the flux of geochemicals as well as the anthropogenic ones, have been discovered. Many have been reported and are the subject of several reviews. They are the result of biological, chemical, and geophysical processes, and most have been verified based on observations in the field and/or in the laboratory. Some have been thoroughly studied while others have not. As a consequence, there are well-developed descriptions for several processes as well as many theoretical equations for the flux. A unified theory is proposed for connecting flux across the interface.

Photographs taken of the interface region, obtained using a sediment profile camera [2, 3] are displayed in Figs. 9.1–9.4. (Figures 9.1–9.4 A collection of color images of the sediment–water interface. These are selected photos taken by Joseph Germano over a time period of 28 years. Four categories are presented.) Fig. 9.1 contains images of the interface and a small sampling of the wide range of effects caused by various macrofauna. Figure 9.2 shows images of the interface being acted upon by submerged aquatic plants with leafy parts in the water column above and holdfasts below. Figure 9.3 has images which indicate an interface under the influence of low oxygen and/or chemical pollutant stresses. Finally, Fig. 9.4 shows the particle advection process. These are but a few glimpses of the character

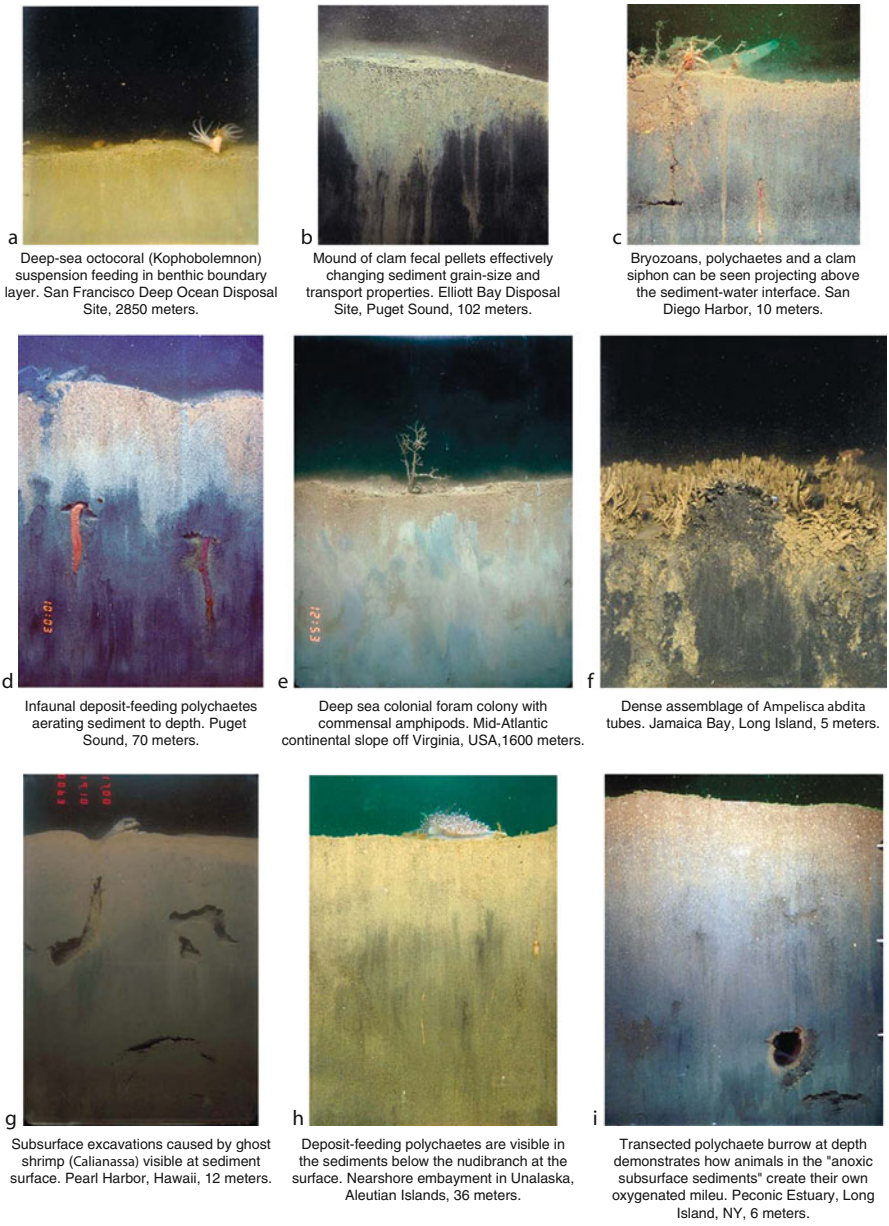

Fig. 9.1 Animal–sediment–fluid relationships (9 photos)

and forms of this important global environmental interface which occupies the largest plane area on Earth. It separates the fluid water–dominated media above and the underlying solid, fluid water–saturated zone below. Figure 9.5 is a conceptual illustration of the interface and its adjoining regions, modified from the original by

a Subsurface infaunal burrows can be seen beneath the fronds of *Caulerpa prolifera* on the sediment surface. Coastal embayment off Sicily, 14 meters.

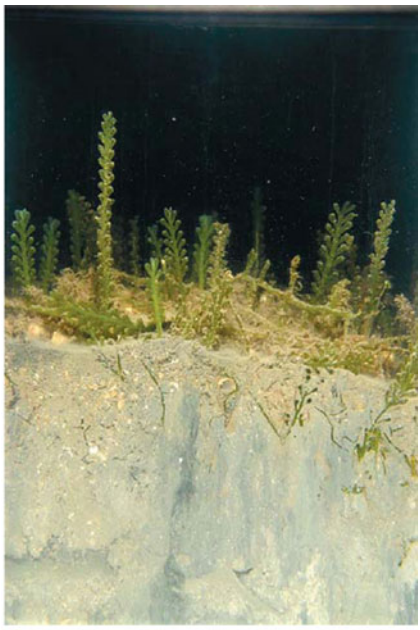

b These sandy clays support a dense assemblage of the invasive *Caulerpa racemosa*. Coastal embayment off Sicily, 8 meters.

c Mixed assemblage of red algae with a frond of *Laminaria* pushed below the sediment surface by the camera prism. Sinclair Inlet, Puget Sound, 5 meters.

d Fronds of seagrass can be seen above these silty fine sands. Sinclair Inlet, Puget Sound, 4 meters.

Fig. 9.2 Submerged aquatic vegetation (4 photos)

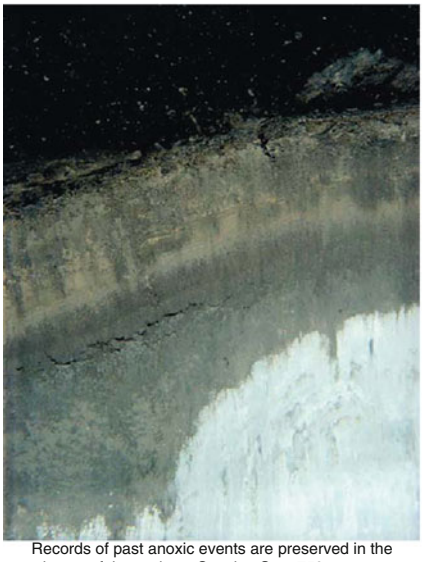

a Records of past anoxic events are preserved in the layers of these clays. Caspian Sea, 750 meters.

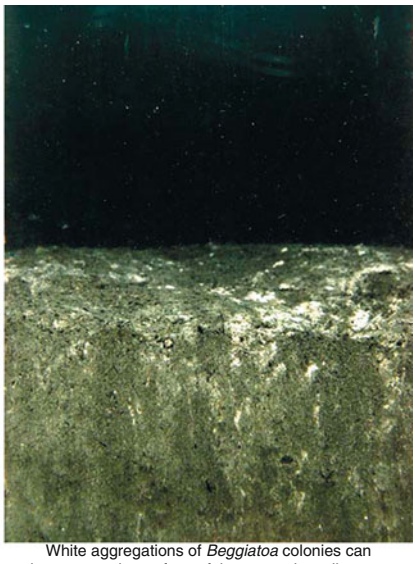

b White aggregations of *Beggiatoa* colonies can be seen on the surface of these anoxic sediments. Nearshore embayment in Unalaska, Aleutian Islands, 32 meters.

c No visible RPD can be seen in these organically enriched sediments. Hackensack River, New Jersey, 3 meters.

d A diffusional layer of oxidized sediment can be seen on the surface of these riverine sediments. Hackensack River, New Jersey, 4.5 meters.

Fig. 9.3 Polluted sediments (4 photos)

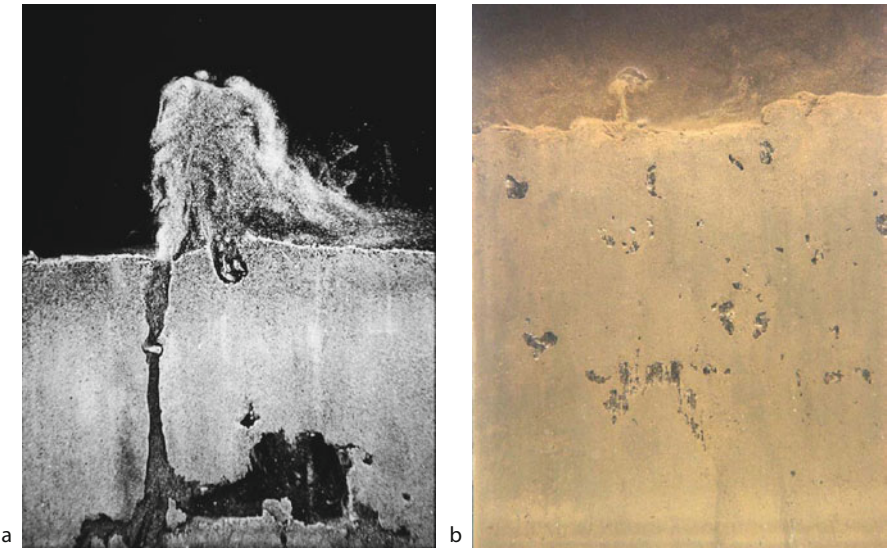

a Deposit-feeding infaunal taxa such as maldanid polychaetes can loosen sediment fabric and eject particles into the benthic boundary layer. Long Island Sound, 15 meters.

b Subsurface methanogenesis can also periodically release gas and sediment particles into the overlying water. Saginaw River , 3 meters.

Fig. 9.4 Examples of particle advection (2 photos)

Santschi et al. [4]. It is an idealized model of the previous images showing the location of the interface plane and some of the processes occurring in the adjoining bulk media phases or compartments.

At any interface locale, it is expected that a combination of individual processes on either side may control the net flux. There may be a dozen or more individual processes, identifying the key ones on either side and coupling them in a logical fashion so as to understand the overall process and quantify the effective flux is an ongoing challenge. As the photographs show, each sediment–water interface has unique characteristics so that the flux is expected to be highly variable from locale to locale. One goal of this chapter is to develop a unified theory for combining the individual processes on the water-side to those on the sediment-side and to obtain the appropriate algorithm for the across-media or interphase flux. The substances of concern are geochemicals such as nitrogen, silica, carbon, and lead and anthropogenic chemicals such as polychlorinated biphenyls, naphthalene, ibuprofen, and caffeine. The development also is applicable to aquasols, nanoparticles, and other identifiable particles moving across the sediment–water interface.

This chapter will first review the available transport processes theories. Several significant individual processes will be listed and summarized. Based on the mechanisms that drive the transport, each will be placed into one of two categories of flux equation types. The theoretical arguments supporting the use of two categories will be covered. Then, a model development section will begin with

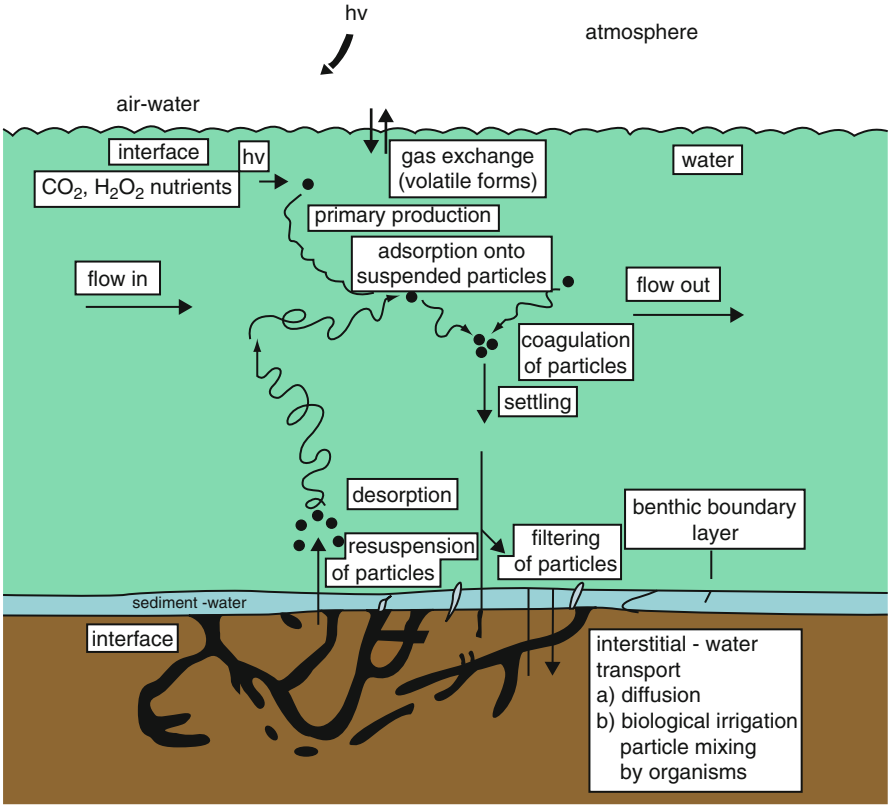

Fig. 9.5 Transport processes near the sediment–water interface. This figure is a slightly modified version of the original produced by Santschi et al. [4]. It is a classical graphical illustration of the interface plane. It is an idealized model of the interface region showing some of the processes occurring in the water column and the bed surface layers

a literature review and summary of the various theoretical approaches proposed for combining the individual processes arriving at the net flux across the interface. The algebraic forms of the flux equations will be given. Finally, the concepts behind the proposed interface compartment (IC) theory will be presented and the flux equation derived. Included will be a discussion of the IC theory in relation to the existing ad hoc protocols in use.

The methods section will describe the modeling approach, the chemicals used in numerical simulations, and the individual processes selected for performing the flux calculations. Including flux calculations in the theoretical section is necessary because it extends and amplifies the IC model theory by providing a layer of reality to accompany the mathematical formulas. In addition, it provides a quantitative means of comparing it to the approaches being used.

Transport Process Theories

There are numerous individual chemical transport processes operating on both sides of the sediment–water interface, and they have been the subject of literature reviews [4–6] and monographs [7–12]. Two types of equations are commonly used that reflect process mechanisms. They are the chemical potential and media advection; one or the other type will be applicable to each process as they are presented and discussed. The chemical potential type will be considered first.

The molecular diffusive transport process derived from Fick's first law of diffusion is the most basic and ubiquitous process [13–15]. The integrated equation is a chemical potential–type process. It contains a concentration difference term that reflects the chemical potential between two locations in space. It also contains an effective diffusion coefficient for the porous medium and the path length. It is applicable to the transport of all solutes and to Brownian particles in bed sediment as well as on the water-side of the interface. On the water-side of the interface, the mass transfer coefficient often replaces the diffusion coefficient and path length quotient [14].

At this juncture, it is well appreciated by the reader that chemical flux, such as molecular diffusion, is a function of the concentration difference or gradient and a kinetic transport parameter. Chemical reactions and phase partitioning can and do occur in the layers on either side of the interface, which affects the magnitude of the respective concentrations and hence the flux. However, applying the transient, reactive-diffusion equation to the chemical species of interest in each layer is beyond the scope of this article. For the sake of clarity, the tactical analytical approach taken in this manuscript portrays the sediment–water interface region so as to isolate and focus only on the transport processes. Therefore, the reader should note that the two layers of interest are assumed to be very thin, void of chemical reactions within (i.e., degradation, oxidation/reduction, polymerization, etc.), and have constant concentration differences across them. In other words, the chemical species are conserved, and a steady-state flux is occurring in the defined sediment–water interface region.

The term Brownian diffusion is conventionally applied to very small particles that respond to the kinetic motions of the surrounding solvent molecules. The transport of colloids, also termed aquasols, in the water on either side of the interface is quantified by a chemical potential–type transport process. These are present in the form of dissolved organic carbon (DOC) particles or inorganic particles with sorbed chemical fractions. The bioturbation transport process of particles in the bed as well as in the adjoining porewater is driven by the presence of macrofauna. It is consistent with the chemical potential–type transport mechanism in that the randomness of a collection of macrofauna-driven particle and fluid motions mimics the molecular kinetic mechanism of diffusion on a larger physical scale. For this reason, it is termed a biodiffusion process and is treated as such mathematically [9, 14, 16–19]. Bioturbation has also been depicted as a convective transport process. This typically involves use of bed turnover rate and nonlocal

particle movement rates. However, the potential-based biodiffusion also has theoretical merit in that the range of macrofauna sizes and transport lengths tends to approach a Gaussian distribution, indicating that the process can be described by a diffusion type of equation. In addition, the biodiffusion model has an extensive database of field- and laboratory-measured biodiffusion transport coefficients that convective transport lacks for this process [19].

The two generic forms of the chemical potential–type flux equations are

$$F = (D/h)\left(C_S - C_i\right) \tag{9.1}$$

and

$$F = K\ \left(C_i - C_w\right), \tag{9.2}$$

where F ($kg/m^2/s$) is the flux, D is the diffusion coefficient (m^2/s), h is the path length (m), K is the convective mass transfer coefficient (m/s), and C (kg/m^3) represents the concentration in water for the sediment bed (s), the interface (i), and the water column (w) beyond the benthic boundary layer, respectively.

The media convective–type rate equation for chemical flux reflects a transport mechanism driven by the directed motion of a bulk media. Several types operate across the interface region. In-bed porewater convection moves solutes and fine particles in both directions. The porewater flow direction responds to hydraulic pressure differences across the bed layers. These can be long-range pressure differences such as in-bank and water column head differences or localized pressure differences generated by the flowing water column as it encounters local bottom roughness such as sand waves, mounds, etc. [20]. In either case, the chemical flux is the product of the effective Darcian porewater velocity and its aqueous concentration.

Solid particles moving through the water-side benthic boundary layer are also a media convective–type flux. The primary ones are particle deposition onto the bed from the water column and resuspension from the bed surface. These transport mechanisms are initiated and maintained by the action of the flowing water. The fluid-generated shear stress at the bed surface drives particle movements into suspension as well as change the particle deposition probability [21, 22]. However, particles and so-called marine snow are also formed in the water column [23], and others originate as wind-blown dust on the sea surface, etc.; all types are deposited onto the bed. The physics of cohesive and noncohesive sediment transport employs complex algorithms for their estimation [24, 25]. For the purpose of this manuscript, a deposition velocity and a resuspension velocity will be used to characterize the respective processes. In each case, the flux is equal to a velocity–concentration product so the generic forms of the media convective–type equation are

$$F = v_w C_w \tag{9.3}$$

and

$$F = v_p C_p, \tag{9.4}$$

where v_w and v_p (m/s) are the effective media velocities of water and particles perpendicular to the interface plane, and C_w and C_p are the media concentrations.

The above review covers the most well-known, characterized, and quantified individual processes. Several other processes have been observed and described. One termed the "benthic cannon" is dramatic and appears in Fig. 9.4. As shown, the organism responsible for this phenomenon (a maldanid polychaete) is seen injecting a spray of fine particles from its burrow into the lower portion of the water column. In a similar mechanism, gas bubbles generated within the bed can also move to the interface and emerge, likewise injecting fine particles into the water-side boundary layer (Fig. 9.4). The role of the nepheloid layer, made up of submerged aquatic vegetation and other macrofauna activities that enhance and attenuate chemical transport processes, remains to be studied and quantified. Due to the lack of sufficient information on these and other individual processes, they cannot be included in numerical simulations at this time.

Several computational studies have been performed aimed at comparing aspects of various individual processes. The most comprehensive of these is a study of trichlorobiphenyl (TCP) for nine in-bed transport mechanisms [26]. Individual processes were ranked by characteristic times-of-recovery of TCP in freshwater riverine bed sediment. It was concluded that in high-energy environments, sediment transport was likely the dominant sediment-side TCP transport process, while in low-energy environments, bioturbation was likely to dominate the movement rate of TCP in the upper layer of the bed. Singh et al. [21] developed a framework for a comprehensive mathematical model for fine and cohesive sediment transport to be combined with contaminant transport models in rivers, lakes, and estuaries; they observed that much research needs to be done before truly realistic chemical exchange models for the sediment–water interface will be available for practical use. They further noted that sediment transport and chemical transport must be meshed in development of a comprehensive model. In assessing the soluble release process of polychlorinated biphenyls (PCBs) from bed sediment in three North American rivers, Thibodeaux et al. [27] evaluated five individual transport processes by comparing the magnitudes of the mass transfer coefficients. However, such individual process studies do not completely address the interconnections that result in across-media transport at the sediment–water interface. Comprehensive studies of the interconnections of transport processes are lacking. A study limited to solute transport of polychlorinated biphenyls in the Hudson River highlights the importance of connecting processes across the interface plane [28, 29]. It was found that during active in-bed bioturbation, the transport resistance on the water-side benthic boundary layer is significant and that both of these processes regulate the PCB flux from the bed.

The number and complexity of the biological, chemical, and geophysical processes cooperating to drive chemical flux across the interface is daunting, and sorting out the cause-and-effect factors is confusing without the aid of theoretical guidance. Ad hoc approaches are in use, but all have theoretical shortcomings and may not, therefore, extend into areas outside of the data set. A robust theory that can accommodate the types of various individual chemical transport processes on either side of the interface and connect them in a logical and transparent procedure is needed for several reasons. In the first place, there appear to be none available. Second, having one will lead to much better understanding of the overall situation related to transport and will provide a hypothesis for interpretation of flux data from both laboratory and field measurements. Third, modelers of aquatic chemodynamic processes need a theory-based procedure for connecting chemical movement between the adjoining bulk-phase compartments based on first principles.

Theories and Model Development

G. S. Ohm (1787–1854) found that the electric current (I) is directly proportional to the difference in voltaic potential between the ends of a conductor (V) and the proportionality constant is R^{-1}, where R is the resistance. G. R. Kirchhoff (1824–1887) extended Ohm's law. By analogy, the Ohm–Kirchhoff laws were applied by Whitman [30] and Lewis and Whitman [1] to chemical flux (F) across a gas–liquid interface plane. The emf potential, V, was replaced by chemical concentration potential such as ($C_s - C_i$), and the result is the well-known resistance-in-series (RIS) law for chemical mass transfer. When applied to the solute at the sediment–water interface the flux equation is

$$F = (C_s - C_w) / \left[\frac{1}{B} + \frac{1}{D}\right], \tag{9.5}$$

where B and D (m/s) are the water-side and sediment-side mass transport coefficients, respectively. Because of chemical-to-water partitioning, with coefficient K_d (L/kg), the $C_s = w_s/K_d$, where w_s (g/kg) is chemical loading on sediment solids and $D = D_b\, \rho\, K_d/h$, where D_b (m^2/s) is the biodiffusion transport coefficient, ρ (kg/L) particle density, and h (m) bed depth. This result has been verified using field data [29, 31].

Resistance-in-series is applicable only to potential-driven processes. It is often time referred to as Ohm's law [32, 33] and has become a shortcut modeling approach. Misapplication occurs, for example, when media velocity is treated as a potential-type transport coefficient and likewise added in the resistance fashion to obtain the overall resistance. It has been misapplied for atmospheric deposition of gases and particles where both potential and convective processes resistances are summed [34, 35]. Hybrid applications that involve converting the chemical

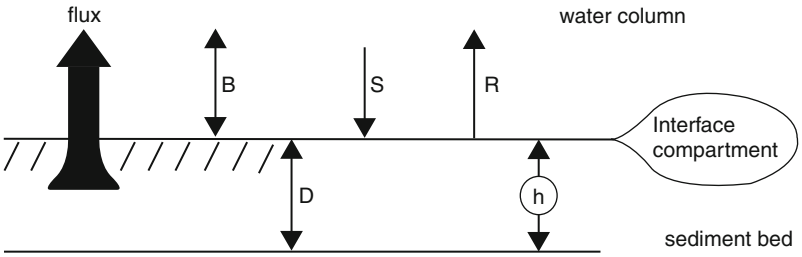

Fig. 9.6 The essence of the interface compartment. The bubble indicates the location of the IC. It is a plane surface so the line depicts one edge. The large arrow to the left depicts the chemical flux and direction. Transport begins in the sediment bed, crosses the interface, and emerges into the water column. This net flux is a result of four individual processes. The B process is solute transport through the water-side benthic boundary layer. The S process is particle deposition (i.e., settling) onto the bed surface and R is particle resuspension from the bed surface. On the sediment side, the D denotes a diffusive process across a distance h. This illustration is used in deriving the IC model equation (i.e., Eq. 9.8)

potential resistance to an equivalent media convective type for use with the adjoining bulk-phase concentrations appear in multimedia compartment (MMC) models [33, 36] for the sediment–water interface. As presented in the next section, a return to first principles embodied in the Ohm–Kirchhoff and Lewis–Whitman laws will mend the problem and produce a unified theoretical construct that accommodates both types individually and in unison.

Environmental models contain multiple phases so interfaces are necessary. The sediment–water interface is depicted as an idealized concept in Fig. 9.5. It is an imaginary plane within the complex transition zones separating bulk water phase from bulk sediment phase as depicted in the Figs. 9.1 to 9.4. The "interfacial compartment" is defined based on the following assumptions and concepts: (a) it is a two-dimensional surface containing no mass that separates the adjoining bulk phases, (b) the chemical flux direction is perpendicular to the surface plane, (c) the net entering and departing fluxes are equal, (d) a hypothetical aqueous chemical concentrations with mass per volume units (mg/m^3) is assumed, and (e) because solid (i.e., particle) phases exist on one side, chemical equilibrium is assumed to exist at the interface plane for estimating the equivalent aqueous concentration. A mass balance on the interface plane is performed. Because of assumption, a steady-state equation results and yields a simple algebraic relationship for the interface compartment concentration. It in turn yields a single flux equation containing the individual process mass transfer coefficients and the bulk chemical concentrations in the adjoining media compartments.

Although there are many individual processes occurring in the region of the interface, for demonstration purpose, only four will be used in the following derivation of the interfacial compartment model. This approach simplifies the mathematics of the theoretical procedure while maintaining the essence of the concept. The combination of chemical potential–type and media convective–type transport mechanisms used is shown in Fig. 9.6. The double-tipped arrows on either

side of the interface are the chemical potential type. They represent respectively the solute transport across the benthic boundary layer with coefficient B (m/s) and diffusive transport within the upper sediment layers with coefficient D/h (m/s), where the layer thickness is h (m). The single-tipped arrows depict the media convective–type flux equations. They represent particle deposition or settling with coefficient S (m/s) and particle resuspension with transport coefficient R (m/s). The assumed chemical movement pathway and direction of flux F ($kg/m^2/s$) is depicted by the large arrow. The sediment bed porewater concentration, C_S (kg/m^3), in equilibrium with the bed load fraction, w_a (mg/kg), is at position h, and the bulk water column concentration is C_W (kg/m^3) and is located at the edge of the benthic boundary layer. The overall chemical potential driving force is the concentration difference, $C_S - C_W$.

A steady-state Lavoisier mass balance for the interface compartment requires that the flux from the sediment-side to the interface, F_{si}, equals that departing the interface on the water-side, F_{iw}. It is

$$F_{si} = (D/h)(C_s - C_i) = B(C_i - C_w) + RC_i - SC_w = F_{iw} \tag{9.6}$$

This result yields the concentration in the interface compartment:

$$C_i = ((D/h)C_s + (S + B)C_w)/(D/h + B + R) \tag{9.7}$$

Combining the two equations yields flux between the compartments in terms of the bulk-phase concentrations:

$$F_{IC} = \frac{C_s(1 + R/B) - C_W(1 + S/B)}{h/D + 1/B + Rh/BD} \tag{9.8}$$

This result is the interface compartment model (IC) flux; it is consistent with the traditional potential flux in that it takes the form of Eq. 9.5 when the convective parameters S and R are set to zero. It is the opinion of the authors that the above procedure is the correct one. However, alternative flux relationships have been proposed for the across-interface flux based on various assumptions and methodologies. Two commonly used approaches appear below.

Invoking the RIS concept directly by mimicking the form of Equation 9.5 is one approach used [32]. In its derivation, the water-side conductances are summed and then inverted to obtain the overall water-side resistance which is then added to the sediment-side resistance. This procedure yields

$$F_{RIS} = \frac{C_s - C_w}{h/D + 1/(B + R - S)} \tag{9.9}$$

for the RIS flux equation. The multimedia compartment or box model approach is a hybrid [33]. Its derivation starts by decomposing chemical potential flux into two

individual convective-type flux components. It then uses the Lavoisier mass balance for summing the individual fluxes but assumes all are driven by the bulk compartment concentrations. The multimedia compartment (MMC) flux equation is

$$F_{MC} = \frac{C_s - C_w}{h/D + 1/B} + (RC_s - SC_w) \tag{9.10}$$

The flux equation for the RIS and MMC models reduce to Eq. 9.5 when S and R are set to zero.

At this juncture, it is clear that three very different algebraic algorithms based on as many approaches are available for estimating the flux across the sediment–water interface. In all cases, the fluxes are linear in relation to the bulk media concentrations and contain the appropriate conductance. Only in the case of the RIS model must the bulk media concentrations be equal for a zero flux. For both the IC model and the MMC model equations, a simple algebraic proof shows that positive, nonzero bulk media concentrations can yield a zero flux. This is a more realistic outcome because in nature it is possible to have a situation where a mix of conductance produces a zero net flux and the bulk media concentration is unequal. Numerical simulations using the theoretical models in flux calculations provide a realistic and quantitative means demonstrating these and other outcomes. The methods used and the results of the numerical flux calculations are presented and discussed in the next section.

Simulation Methods and Results

Although only four individual transport processes were used in the development of the three theoretical models presented in the previous section, nine individual transport processes will be used in the numerical simulation. This is done in order to realistically mimic and highlight the most significant process typically present in the sediment–water interface region. The four on the water-side include solute transport in the benthic boundary layer, particle resuspension from the bed surface, particle deposition from the water column onto the surface, and colloid Brownian transport through the benthic boundary layer. The five on the bed-side are colloid Brownian diffusion in the porous bed, Darcian water advection into and out the bed, solute molecular diffusion in porewater, particle biodiffusion, and porewater biodiffusion. Altogether, there are five chemical potential–type flux expressions and five media advection type. The types and categories of the processes plus the base case numerical values of the parameters are summarized in Table 9.1. The top four lines represent the water-side transport coefficients and the remaining six represent the bed-side transport coefficients. The large numerical difference in the PCB versus BZ transport coefficients are due to partitioning for the particle-associated processes. For details on how the bed and water column transport

Table 9.1 Transport coefficients (m/day)

Name, location, and type[a]	Benzene	PCB
Solute, water-side mass transfer coefficient, cp.	0.32	0.30
Particle resuspension, ma.	5.72E-5	1.24
Particle deposition, ma.	2.0E-9	4.32E-5
Colloid, water-side, ma.	2.31E-7	4.99E-3
Colloid, bed-side, cp.	2.31E-4	2.31E-4
Darcian velocity into bed (−), ma.	4.35E-4	3.99E-4
Darcian velocity from bed (+), ma.	1.18E-3	1.08E-3
Solute diffusion in bed, cp.	7.48E-4	6.85E-4
Particle biodiffusion, cp.	1.14E-5	0.25
Porewater biodiffusion, cp.	2.0E-4	2.0E-4

[a]*cp* chemical potential, *ma* media advection–type flux

coefficients are calculated, see Chapters 10 through 13 in the *Handbook of Chemical Mass Transport in the Environment* [37].

Data available in the literature on several North American rivers and lakes with bed sediment and water column contaminated with organic chemicals were used. Several studies [27, 29, 38–41] provide the necessary physical, chemical, and biological data and information needed for estimating the bed and water column transport coefficients used in the calculations. Typical bed and water column characteristics at 25°C and 3 m water column depth were used. These characteristics were bed porosity, 75%; bulk density, 572 kg/m^3; sediment layer thickness for active transport, 0.05 m; fraction organic carbon in bed solids, 50 g/kg; dissolved organic carbon (DOC) in the porewater, 50 g/m^3; particle biodiffusion coefficient, 2E-6 m^2/day; porewater biodiffusion coefficient, 2E-5 m^2/day; colloid Brownian diffusivity, 1.61E-5 m^2/day; Darcian water convection into bed, 4E-4 m/day, and out, 1.1E-3 m/day; Peclet number = 1; water column suspended particle concentration, 0.005 kg/m^3; particle deposition velocity, 4E-4 m/day; particle resuspension velocity, 1E-4 m/day; and colloid benthic boundary layer transport coefficient, 2.3E-4 m/day.

The porewater chemical concentrations are separated into dissolved and particle-bound DOC fractions and the fractions transported separately, the dissolved as solute molecular diffusion and the DOC as Brownian particle diffusion. The chemical equilibrium phase distribution partition coefficient is used to relate the solute and DOC-bound concentrations. For characterizing the physical properties of the bed, the New Bedford Harbor estuary site was used [41]. The chemical 2,4,2',4'-tetrachlorobiphenyl was used as the PCB. Its partition coefficient was 21.6 m^3/kg and that used for benzene (BZ) was 0.001 m^3/kg. The tabulated molecular diffusivity in water for each was used [14]. For the benthic boundary layer, solute transport coefficients were based on those from the Hudson River; they were 0.32 and 0.30 m/day for BZ and PCB, respectively. These two chemicals represent the extremes of hydrophobic properties typically encountered in contaminated bed sediments. In addition, they also represent the extremes of numerous soluble and particle-phase geochemicals.

Table 9.2 PCB flux ($g/m^2 \cdot d$) increasingly active processes

Active processes				
C_s =.065, C_w =.020	$C_i(g/m^3)$	IC	RIS	MMC
1. Mol. diff., bed porosity 0.1%	.020	4.3E-9	4.3E-9	5.0E-8
2. Mol. diff., bed 78% porosity	.021	3.1E-5	3.1E-5	3.18-5
3. Water advection into bed, Pe = −10	.0196	−1.3E-4	−2.8E-3	−4.1E-4
4. Mild resuspension, Pe = +10, DOC on.	.0195	4.5E-4	3.3E-4	2.4E-3
5. Aggressive resuspension	.00418	4.5E-4	3.4E-4	8.1E-2
6. "Storm event" resuspension	.00013	4.5E-4	3.4E-4	3.2
7. Mild resusp., mild in-bed biodiff.	.0468	9.4E-3	9.0E-3	1.1E-2
8. Mild resusp., aggressive biodiff.	.0648	1.5E-2	1.5E-2	1.6E-2
9. "Storm" resusp., aggressive biodiff.	.0413	2.1	1.4	3.2

The data appearing above were used with the appropriate algorithms and formulations to estimate the numerical values of the nine transport coefficients [14]. Water (porewater in the bed and in the column above) is the continuous phase across the interface. The transport coefficients use chemical concentrations in water for flux calculations with both the chemical potential–type and media advection–type equations. A summary of typical numerical values of the nine transport coefficients appear in Table 9.1 for BZ and PCB. Several of the base-case transport parameters were perturbed in doing numerical simulations to cover their expected range of variation.

The results of the first numerical study appear in Table 9.2. Calculated fluxes for the PCB using the three theoretical models, the interface compartment (IC) model, resistance-in-series (RIS) model, and multimedia compartment (MMC) model, appear. In addition, the IC model interface concentration, C_i (g/m^3), is given. This simulation uses a porewater concentration of 0.065 g/m^3 and water column 0.020 for a chemical potential gradient driving the PCB flux from the bed to the water column for positive flux values with unit $g/m^2 \cdot d$. The negative values denote fluxes directed into the bed. The first numerical study was to assess the role of transport aggressiveness or intensity on the flux.

The first three simulations (i.e., 1, 2, and 3) represent molecular diffusion and in-bed water advection. The flux varies from low positive to negative. Low bed porosity will produce a low flux; all models have essentially the same values for simulation 2. Porewater advection in the opposite direction is sufficient to reverse flux direction as shown in simulation 3. This reverse in flux behavior is present in all three models, but flux numbers are different for each. This is expected because the algebraic forms are different (see Eqs. 9.8, 9.9, and 9.10).

These IC model simulations reveal an interconnection between the media convective–type erosion process on the water-side and the chemical potential–type diffusive process in the bed (see simulations 4, 5, and 6). In the absence of biodiffusion, which is the case for these three simulations, the flux for the IC and RIS models remains unchanged with increasing particle resuspension aggressiveness. This occurs because the in-bed transport

processes are slow; they are combined porewater advection and molecular diffusion. The resistance-in-series law is operating properly in the IC and RIS models, where the slowest process controls. However, an equivalent resistance-in-series functionality is absent in the MMC model, and the flux tracks particle resuspension directly, resulting in substantially higher fluxes. The generally higher MMC model flux values are due to the porewater solute concentration because it, rather than the interface concentration, is the driver and is always numerically larger.

More interesting process interconnections are revealed in simulations 7, 8, and 9. In these cases, in-bed particle and porewater biodiffusion are active as well as particle resuspension. The flux increases for both the IC and RIS model simulations as they track the level of biodiffusion; however, the MMC model does not change much because it is already high. This behavior by the IC and RIS models shows that an active bed-side process must be present to provide chemical mass readily available and in the upmost layer in order for erosion to be an effective transport process. The rapid biodiffusion provides the mass while the slower molecular diffusion and water advection processes cannot. Finally, all three models give high and approximately equal flux for the most aggressive resuspension and biodiffusion transport coefficients (see simulation 9).

To summarize, the simulation study starts with mild in-bed passive molecular diffusion and a very low-porosity sediment layer. The flux is very low. As one moves down the table, level of transport aggressiveness increases. The final one is for aggressive particle biodiffusion and hydraulic flows that result in aggressive particle resuspension. The flux is very high in this case. The variation in flux from low and high is approximately 10^9. The flux numbers for the IC and RIS models are similar in magnitude while the MMC is consistently higher and, in some cases, much higher. Its flux behavior seems to track the particle resuspension process in aggressiveness. Clearly, Eq. 9.10 supports this behavior.

The flux behavior of BZ is somewhat different; no tabular data are provided. The behavior for simulations 1, 2, and 3 are similar to the PCB ones. Low porosity yields low flux, and into bed water advection can reverse the weak diffusion-driven flux. Being less hydrophobic, BZ displays limited sorption to their surfaces. For this reason the in-bed particle transport is not a significant chemical mobilization process for BZ. For simulations 2 through 9, all three models give essentially the same numerical flux values. All models reflect no particle process dependence, and all display only chemical potential flux–driven behavior patterns. Theoretically, in the absence of particle processes, all three models are equal and become identical to Eq. 9.5.

The second numerical study was on the in-bed concentration gradient difference polarity and the effect on the direction of the flux. Equations 9.8, 9.9, and 9.10 show each model has a different mathematical dependence on the porewater and water column concentration. In the above simulations, the concentration difference was set to simulate chemical transport from the bed, so for PCB, the concentration differences as C_s were =.065 and 0.02 g/m^3, and for BZ, they were 20 and 2.0 g/m^3. So as to further test the models for realistic flux behavior characteristics, the

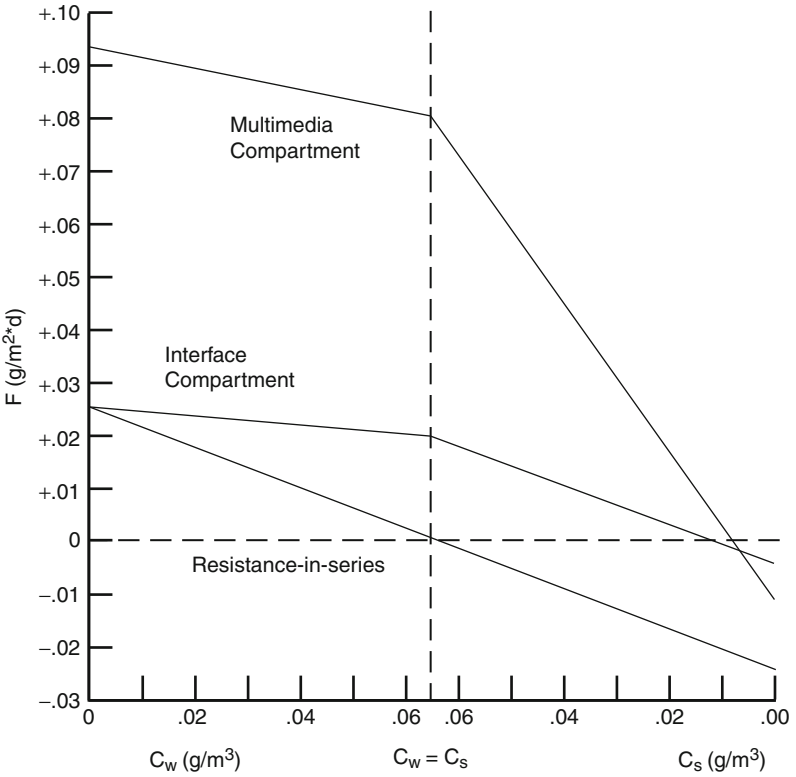

Fig. 9.7 PCB flux across the sediment–water interface. A positive flux, F, is from the bed to the water column and negative is from water to the bed. The concentration differences between bed and water column used in the calculations are displayed on the ordinate. The progression of concentration difference values was devised to force the chemical potential out the bed, on the left, and into the bed on the right so as to drive the flux accordingly. At the vertical dotted line, bed and water concentrations are equal. Only for the RIS model is the flux zero. The three lines depict the theoretical behavior of the PCB flux for the three models: IC, RIS, and MMC

chemical potential gradient range and the direction were reversed; the flux results for reversing the gradient direction appear in Figs. 9.7 and 9.8. In each figure, the flux is on the vertical axis and the imposed concentration difference on the horizontal axis. Each line in Fig. 9.7 represents a model from top to bottom; they are MMC, IC, and RIS.

Figure 9.7 presents aspects of the flux behavior. The vertical axis displays the flux. Positive numbers represent the PCB moving from the bed to the water column. Negative numbers represent the PCB moving from the water column to the bed. The zero flux indicates no net chemical movement in either direction. The horizontal axis displays chemical concentrations in the water column and the porewater. It is an unusual axis in that it has zero on each end and maximum in the center. The horizontal axis consists of two sections divided vertically by a dotted line.

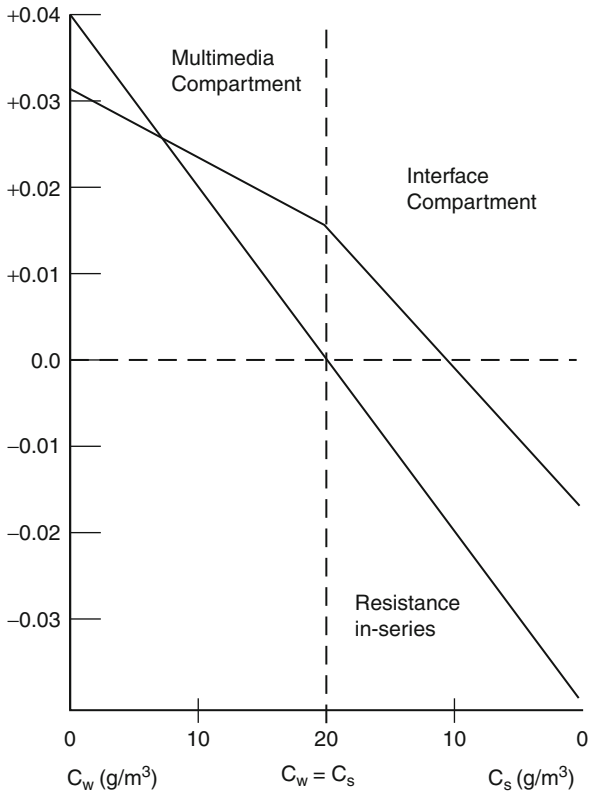

Fig. 9.8 Benzene flux across the sediment–water interface. A positive flux, F, is from the bed to the water column and negative is from water into the bed. The concentration differences between bed and water column used in the calculations are displayed on the ordinate. The progression of concentration values were devised to force the chemical potential out the bed, on the left, and into the bed on the right, so as to drive the flux accordingly. The two lines depict the theoretical behavior of the BZ flux for the three models: IC, RIS, and MMC. The IC and MMC flux values overlap

The concentration is a maximum at the position of the dotted line. To the left side of the vertical line, the porewater concentration in the bed, C_S, is held constant at a value of 0.065 g/m^3 and the water column concentration, C_W, is varied from 0.0 to 0.065 g/m^3 as shown. Under these conditions, the concentration difference tends to move the PCB from the bed to the water column and produce a positive flux. It does for all three models. Only for the RIS model does the flux equal zero for the condition where $C_S = C_W = 0.065$. Due to the particle resuspension process, the PCB flux result for both the IC and MMC models remain positive and nonzero when moving from the bed to the water column. In the next simulation, concentration levels in bed porewater versus the water column concentration will be reversed.

Consider concentration conditions to the right of the dotted line in Fig. 9.7. As shown on the horizontal axis, the water column concentration, C_W, is held constant at 0.065 g/m^3 and the porewater concentration, C_S, is reduced from 0.065 down to 0.0 g/m^3. The flux for the RIS model starts at zero and goes negative as the PCB moves into the bed. The other model results display a positive flux at the start and both trends downward. The MMC model shows a steep decline and reaches zero flux at C_S of about 0.01 g/m^3. The IC flux declines to the same value as well, and this occurs because the imposed concentration gradient encourages PCB movement from the water column to bed.

The point of the above flux versus concentration study for PCBs was to show the different behavior patterns produced by the three models. The horizontal concentration axis was contrived to force the flux to range in magnitude from positive to negative and therefore cover all possible conditions to be encountered in nature. The IC model is theory-based, and so it characterizes the correct PCB flux behavior. Hopefully, future experiments will be able to verify or refute this behavior. The RIS model predicts lower flux values while those for the MMC model are much higher. All three models behave according to the algebraic forms of 9.8, 9.9, and Eqs. 9.10 for the IC, RIS, and MMC, respectively. Both the IC and the MMC models have a flux inflection; this suggests they are better quantitative representations of the overall flux process. Crossing the $C_w = C_s$ line and interchanging concentration represents a switching of processes; it is in the algebra (see Eqs. 9.8 and 9.10).

A somewhat different behavior occurs for BZ. The results are displayed in Fig. 9.8 where the graph is constructed similar to that for PCB. The RIS and MMC flux values are identical and appear as a single diagonal line that starts positive, goes to zero, and then ends negative. The IC model starts at a slightly lower positive flux. It decreases then goes through a slope change at $C_S = C_W$. This is an algebra-driven inflection point in the IC model; it occurs at $C_S = C_W = 20$ g/m^3 (see Eq. 9.8). As C_S decreases toward zero, the flux goes into a steep decline with increasing negative values. It parallels the behavior of the RIS and MC models but with slightly higher flux values. Beyond the IC model, flux is higher than the others. The particle transport process is low, and the MMC model takes the same algebraic form as the RIS. However, the IC model reflects the correct theoretical approach and displays a very different behavior pattern. Being water soluble, BZ has minimal particle association. However, the particle processes enter as ratios (see Eq. 9.8). This has the effect of delaying the zero flux. It occurs at C_S of 11.0 g/m^3.

The flux results for the IC versus RIS and MMC models using this specific simulation with BZ and PCB are different numerically. They also display different behavior patterns as the imposed concentration gradient condition is changed to encourage chemical movement from the bed to a condition of chemical movement into the bed. Presumably, the IC model result is the correct one since it is theory-based. However, at this juncture, it is a hypothesis in need of testing against laboratory and field experimental measurements.

Significance for Aquatic Environments

There are numerous individual transport processes on both sides of the interface that are driven by biological, chemical and geophysical phenomena. Some processes work in parallel while others work in series, forming a connected network of processes moving anthropogenic substances and geochemicals across the interface. The interface compartment (IC) concept and associated mathematical model is developed and presented as the appropriate theoretical approach for understanding the overall process and quantifying the resulting net flux. For aquatic researchers, it is a tool with several uses. It provides a testable hypothesis and a means of interpreting rate data based from measurements in the laboratory or field. It provides a mathematical rate equation for individuals making numerical flux estimates. Finally, the derivation provides a protocol for obtaining one additional model equation for use by chemical fate modeler's connecting mobility across the interface that separates the adjoining bulk sediment and water compartments.

Future Directions

The sediment–water interface is the largest plane surface on Earth. Understanding and quantifying chemical and particle mobility across this semipermeable interface is relevant to the work of a broad community of aquatic researchers. The interface compartment model provides the basic theory for connecting chemical flux across the sediment–water interface. Correctly quantifying the net chemical, particle, and aquasol exchange rates across this plane is a key factor for understanding the fate of numerous natural and anthropogenic substances on Earth and aid in assessing the ecological significance. The potential impact of the IC model's further development and use in the environmental and geosciences fields may be a key contributing factor. Life-forms residing on both sides, in the water column or the surface sediment layers, depend on oxygen and nutrient fluxes. The bed is a source or a sink of soluble and particulate carbon compounds depending on the chemodynamics of the specific locale. The bed is a sink for chemical pollutants entering the aquatic system but, later as conditions improve in the water column, it becomes the source. These are just a few examples of the types of possible uses which require theoretically sound and verified science-based tools. As outlined above, further work is needed on the interface compartment concept before it is accepted as a unified theory and modeling protocol.

Bibliography

1. Lewis WK, Whitman WG (1924) Principles of gas absorption. Indust Eng Chem 16:1215–1220
2. Rhoads DC, Germano JD (1982) Characterization of benthic processes using sediment profile imaging: An efficient method of remote ecological monitoring of the seafloor (REMOTS™ System). Mar Ecol Prog Ser 8:115–128

3. Rhoads DC, Germano JD (1986) Interpreting long-term changes in benthic community structure: a new protocol. Hydrobiologia 142:291–308
4. Santschi P, Hohener P, Benoit G, Brink MB (1990) Chemical processes at the sediment-water interface. Mar Chem 30:269–315
5. Duursma EK, Smies M (1982) Sediments and transfer at and in the bottom interfacial layer. In: Kullenberg G (ed) Pollutant transfer and transport in the sea, vol II. CRC Press, Boca Raton, pp 101–137
6. Krantzberg G (1985) The influence of bioturbation on physical, chemical and biological parameters in aquatic environment – a review. Environ Pollut (Ser A) 39:99–122
7. DiToro DM (2001) Sediment flux modeling. Wiley, New York
8. Kullenberg G (ed) (1976) Pollutant transfer and transport in the Sea-II. CRC Press, Boca Raton
9. Boudreau BP, Jorgensen BB (eds) (2001) The benthic boundary layer. Oxford University Press, New York
10. McCave IN (ed) (1976) The benthic boundary layer. Plenum, New York
11. Windom HL, Duce RA (1976) Marine pollutant transport. Lexington, Lexington
12. Tenore KR, Coull BC (eds) (1980) Marine benthic dynamics. University of South Carolina Press, Columbia
13. Fanning KA, Manheim FT (eds) (1982) The dynamic environment of the ocean floor. Lexington Books, Lexington
14. Thibodeaux LJ (1996) Environmental chemodynamics. Wiley, New York
15. Lerman A (1979) Geochemical processes water and sediment environments. Wiley, New York
16. Boudreau BP (1997) Diagenetic models and their implementation. Springer, Berlin
17. Schink DR, Guinasso NL Jr (1975) Modeling the influence of bioturbation and other processes of $CaCO_3$ dissolution at the sea floor. In: Andersen NR, Malahoff A (eds) The fate of fossil fuel CO_2 in the oceans. Plenum, New York, pp 375–399
18. Berner RA (1980) Early diagenesis. Princeton University Press, Princeton
19. Thibodeaux LJ, Matisoff G, Reible DD (2010) Bioturbation and other sorbed-phase transport processes in surface soils and sediment. In: Thibodeaux LJ, Mackay D (eds) Handbook of chemical mass transport in the environment. CRC Press, Boca Raton (Chap 13)
20. Thibodeaux LJ, Wolfe JR, Dekker TJ (2010) Advective porewater flux and chemical transport in bed-sediment. In: Thibodeaux LJ, Mackay D (eds) Handbook of chemical mass transport in the environment. CRC Press, Boca Raton (Chap 11)
21. Singh VP, Reible DD, Thibodeaux LJ (1988) Mathematical modeling of fine sediment transport. Hydrol J IAH 11:1–3
22. Lick W (2009) Sediment and contaminant transport in surface waters. CRC Press, Boca Raton
23. Lohmann R, Dachs J (2010) Deposition of dissolved and particle-bound chemicals from surface ocean. In: Thibodeaux LJ, Mackay D (eds) Handbook of chemical mass transport in the environment. CRC Press, Boca Raton (Chap 17)
24. Yang CT (2003) Sediment transport. Krieger, Malabar
25. DePinto JV, McCulloch RD, Redder TM, Wolfe JR, Dekker TJ (2010) Deposition and resuspension of particles and associated chemical transport across the sediment-water interface. In: Thibodeaux LJ, Mackay D (eds) Handbook of chemical mass transport in the environment. CRC Press, Boca Raton (Chap 10)
26. Reible DD, Valsaraj KT, Thibodeaux LJ (1991) Chemodynamic models for transport of contaminants from sediment beds. In: Hutzinger O (ed) The handbook of environmental chemistry, part F, vol 2. Springer, Berlin, pp 186–228
27. Thibodeaux LJ, Reible DD, Valsaraj KT (2002) Non-particle resuspension chemical transport from stream beds. In: Lipnick RL, Mason RP, Phillips ML, Pittman CU Jr (eds) Chemicals in the environment, vol 806, ACS symposium series. American Chemical Society, Washington, DC, pp 130–149
28. Thibodeaux LJ, Valsaraj KT, Reible DD (2001) Bioturbation–driven transport of hydrophobic organic contaminants from bed sediment. Environ Eng Sci 18:215–223

29. Erickson MJ, Turner CL, Thibodeaux LJ (2005) Field observation and modeling of dissolved fraction-sediment-water exchange coefficients for PCBs in the Hudson River. Environ Sci Technol 39:549–555
30. Whitman WG (1923) The two-film theory of gas absorption. Chem Metall Eng 29:146–148
31. Thibodeaux LJ, Bierman VJ (2003) The bioturbation-driven chemical release process. Environ Sci Technol 1:253A–258A
32. Monteith JL, Unsworth M (1990) Principles of environmental physics. Butterworth-Heinemann, Oxford
33. Mackay D (2001) Multimedia environmental models. Lewis, Boca Raton
34. Slinn WGN (1978) 4-Wet and dry removal processes. In: NRC (ed) The tropospheric transport of pollutants and other substances to the oceans. National Academy of Sciences, National Academy Press, Washington, DC
35. Trapp S, Matthies M (1998) Chemodynamics and environmental modeling. Springer, Berlin
36. Van de Meent D (1993) Simple box: a generic multimedia fate evaluation model. RIVM Report No. 6727200001. Bilthoven
37. Thibodeaux LJ, Mackay D (eds) (2010) Chapters 10,11,12,13 &17. In: Handbook of chemical mass transport in the environment. CRC Press, Boca Raton
38. Thoma GJ, Koulermos AC, Valsaraj KT, Reible DD, Thibodeaux LJ (1991) The effect of pore-water colloids on the transport of hydrophobic organic compounds from bed sediments. In: Baker RA (ed) Organic substances in water, vol 1, Humics and soils. Lewis, Boca Raton
39. Valsaraj KT, Thibodeaux LJ, Reible DD (1997) A quasi-steady-state pollutant flux methodology for determining sediment quality criteria. Environ Toxicol Chem 16:391–396
40. Savant SA, Reible DD, Thibodeaux LJ (1987) Convective transport within stable river sediments. Water Resour Res 23:1763–1768
41. Thibodeaux LJ, Reible DD, Bosworth WS, Sarapas LC (1990) A theoretical evaluation of the effectiveness of capping PCB contaminated New Bedford Harbor bed sediments. Final Report. HSRC. Middelton Library, Louisiana State University, Baton Rouge